Inorganic Chemistry

Article

pubs.acs.org/IC

Series of Lead Oxide Hydroxide Nitrates Obtained by Adjusting the pH Values of the Reaction Systems

Genxiang Wang,[‡,†] Min Luo,[†] Ning Ye,*[,†,‡] Chensheng Lin,[†] and Wendan Cheng[†]

[†]Fujian Institute of Research on the Structure of Matter, Key Laboratory of Optoelectronic Materials Chemistry and Physics, Chinese Academy of Sciences, 155 W. Yangqiao Road, Fuzhou, Fujian 350002, P. R. China

[‡]College of Chemistry & Chemical Engineering, Fuzhou University, Shangjie Town, Minhou County, Fuzhou, Fujian 350108, P. R. China

Supporting Information

ABSTRACT: A series of lead(II) nitrates have been synthesized by a hydrothermal method and adjusting the pH values of the reaction systems. $Pb_{20}O_6(OH)_{16}(NO_3)_{12}$ and $Pb_2O(OH)NO_3$, crystallize in the centrosymmetric space group $P\bar{1}$ and *Pbca*, respectively. The structure of $Pb_{20}O_6(OH)_{16}(NO_3)_{12}$ features infinite cationic chains of $[Pb_{20}O_6(OH)_{16}]_\infty$ running along *c* axis, and the nitrate groups as the counterions reside between adjacent chains, while the structure of $Pb_2O(OH)NO_3$ can be described as alternate stacking of cationic $[Pb_2O(OH)]_\infty$ layers with anionic $[NO_3]^-$ layers along [001] direction by the weak Pb−O bonds, forming a 3D framework with 1D tunnels of 12-member rings (MRs). $[Pb_4(OH)_4](NO_3)_4$, crystallizing in the noncentrosymmetric space group *Cc*, has been studied as the nonlinear optical material for the first time. The second harmonic generation (SHG) measurement indicates that the SHG responses of $[Pb_4(OH)_4](NO_3)_4$ are 0.7 times that of KDP. Theoretical calculations confirmed the SHG efficiency of $[Pb_4(OH)_4](NO_3)_4$ originates from the cooperative effect of NO_3^- groups and lead oxygen polyhedras in the structure. Meanwhile, the relationship between pH value and ratio of Pb/OH^- in the molecules presents a positive correlation, which results in the diversity of these structures under different pH value.

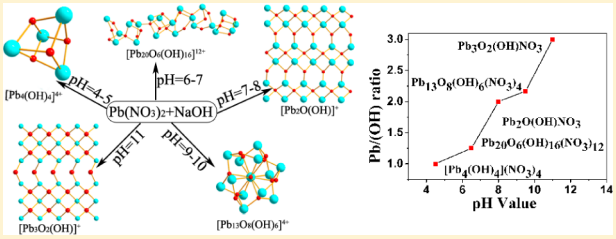

INTRODUCTION

Nonlinear optical (NLO) materials are of great interest for promising applications, including frequency conversion, optical parameter oscillator (OPO), and signal communication, etc.[1−15] Also, searching for NLO crystals with excellent properties has long been targeted in the field of laser science and technology in the past few decades. Currently, a large number of NLO crystals presenting good performance, such as LBO,[16] BBO,[2] and KBBF,[17] have been discovered, some of which have been commercially manufactured and broadly used. Most of the NLO crystals reported recently are borates. On the basis of the anionic groups, the planar $[BO_3]^{3-}$ anionic group, with a moderate birefringence and a large microscopic second-order susceptibility β, is the extremely suitable basic structural unit of NLO crystals for large second harmonic generation (SHG). Analogously, $[CO_3]^{2-}$ and $[NO_3]^-$ groups having the akin planar triangle structure with π-orbitals are expected to be good NLO-active anionic groups as well. Recently, apart from borates, the synthesis of carbonate crystals has also drawn much attention. Such crystals presented lately are $CsPbCO_3F$,[18] $ABCO_3F$ (A = K, Rb, Cs; B = Ca, Sr, Ba),[19] $Na_8Lu_2(CO_3)_6F_2$, $Na_3Lu(CO_3)_2F_2$,[20] and $K_{2.70}Pb_{5.15}(CO_3)_5F_3$.[21] However, few nitrates with SHG performance have been reported for its large water solubility.[22,23] Thus, it is a big challenge to find nonaqueous or low-soluble nitrates as the NLO materials. On account of the ideal planar triangle structure $[NO_3]^-$ ions in nitrates, some potential new NLO materials of nitrates may be discovered. Besides the planar triangle $[NO_3]^-$ group, a general strategy for synthesizing new NLO materials is to employ noncentrosymmetric (NCS)[24,25] chromophores as building units which consist of distorted polyhedra with a d^0 cation center resulting from a second-order Jahn−Teller effect,[26−28] polar displacement of a d^{10} cation center,[29,30] or distortion from the stereochemically active lone pair effect of the cation,[31] or borate p-orbital systems. It has been demonstrated that the combination of the above two types of polarization groups can produce compounds with excellent SHG properties such as $Pb_2B_5O_9I$,[32] $BaMo_2TeO$,[26] and $BaNbO(IO_3)_5$.[33] Therefore, we expect that the combination of Pb polyhedra and the planar triangle $[NO_3]^-$ group may produce new NLO materials.

An examination of the literature about lead nitrates reveals that several studies about basic lead nitrates have been carried out.[34−40] The speciation of lead−hydroxo moieties plays an important role in understanding the mechanism of transport of lead in aqueous systems.[37−41] The earlier studies for basic lead nitrates mainly focused on studying the resultant precipitates in the aqueous system $Pb(NO_3)_2$−NaOH by using conductometric and potentiometric titrimetry coupled with chemical analysis and solubility-product determinations or powder X-ray

Received: February 20, 2014
Published: May 5, 2014

   dx.doi.org/10.1021/ic5004116 | *Inorg. Chem.* 2014, 53, 5222−5228

diffraction methods, and some empirical formulas, such as $Pb(NO_3)_2{\cdot}Pb(OH)_2$, $Pb(NO_3)_2{\cdot}5PbOH)_2$, $2Pb(NO_3)_2{\cdot}5Pb(OH)_2$, and $Pb(NO_3)_2{\cdot}3Pb(OH)_2$, were obtained.[34−36] Subsequently, studies about the category of basic salt phase in aqueous nitrate solutions with different pH values have been reported, and some crystal structures of basic lead nitrate have been successively reported.[37−41] Because of the fact that, in aqueous solutions, Pb^{2+} cations usually form polynuclear complexes with Pb^{2+}cations linked via bridging hydroxyl groups and/or oxygen atoms, various lead−(oxide, hydroxide) clusters have been discovered.[38,37−41] In these clusters, anions (O^{2-} or OH^-) play the role of the central atom. Generally, the O^{2-} anion is located at the center of a tetrahedron defined by Pb^{2+} cations, thus forming (OPb_4) oxocentered tetrahedra. (OPb_4) tetrahedra may polymerize by sharing edges and vertices to form polyions of different connectivity and dimensionality.[41−43] Also, the types of clusters relate to the pH values in the reaction system, which is significant in understanding the transport of lead and the crystallization of lead compounds in natural systems. The empirical formulas and some of these structures of the reported lead oxide hydroxide nitrates have been summed up according to their $Pb:NO_3$ elemental ratio.[41]

In view of a literature study, for more systematically understanding the relationship between pH value and type of crystals containing lead−(oxide, hydroxide) clusters, the $Pb(NO_3)_2$−NaOH system was studied by hydrothermal method and single crystal X-ray diffraction method. In the exploratory synthetic work to date, five lead oxide hydroxide nitrate species were obtained by simply adjusting the pH values in the reaction system of $Pb(NO_3)_2$ aqueous solution under subcritical hydrothermal conditions, including previously reported compounds, $[Pb_4(OH)_4](NO_3)_4$,[37] $Pb_{13}O_8(OH)_6(NO_3)_4$,[39] and $Pb_3O_2(OH)NO_3$,[40] which was previously reported with an accentric space group, $Pca2_1$. However, the space group of $Pb_3O_2(OH)NO_3$ has been confirmed to be a centrosymmetric space group, *Pbcm*. There are no reports about the NLO properties in the literature for the acentric one, $[Pb_4(OH)_4](NO_3)_4$. Details of the syntheses, crystal structures, the relationship between the category of obtained compounds and conditions of reaction system, thermal behavior, optical properties, and NLO properties of $[Pb_4(OH)_4](NO_3)_4$ are presented in this work.

EXPERIMENTAL SECTION

Reagents. $Pb(NO_3)_2$ (AR,99.0%) and NaOH (AR,99.0%) were purchased from Sinopharm.

Syntheses. Crystals of $[Pb_4(OH)_4](NO_3)_4$, $Pb_{20}O_6(OH)_{16}(NO_3)_{12}$, $Pb_2O(OH)NO_3$, and $Pb_3O_2(OH)NO_3$ were grown by solvothermal techniques using a mixture of $Pb(NO_3)_2$ (1.656 g, 0.005 mol) and H_2O (10 mL) with the addition of the NaOH 0.100 g (0.0025 mol), 0.250 g (0.0065 mol), 0.300 g (0.0075 mol), and 0.400 g (0.01 mol), respectively, and were sealed in the autoclaves equipped with a Teflon liner (23 mL) and heated at 220 °C for five days, followed by slow cooling to room temperature at a rate of 5 °C /h, and the final pH values are about 4−5, 6−7, 7−8, and 11, respectively. Colorless rhomboid crystals of $[Pb_4(OH)_4](NO_3)_4$ were collected in a yield of about 90% based on Pb. Colorless long striped crystals of $Pb_{20}O_6(OH)_{16}(NO_3)_{12}$ were collected in a yield of about 95.2% based on Pb. Pale yellow flaky crystals of $Pb_2O(OH)NO_3$ were collected in a yield of about 96.4% based on Pb. Colorless thin columnar crystals of $Pb_3O_2(OH)NO_3$ were collected in a yield of about 60%. All the four reaction products, nonaqueous at room temperature, were washed with deionized water and ethanol.

Single Crystal Structure Determination. Single crystal X-ray diffraction data for $[Pb_4(OH)_4](NO_3)_4$, $Pb_{20}O_6(OH)_{16}(NO_3)_{12}$, $Pb_2O(OH)NO_3$, and $Pb_3O_2(OH)NO_3$ were collected at room temperature on a Rigaku Mercury CCD diffractometer with graphite-monochromatic Mo Kα radiation (λ = 0.71073 Å). A transparent block of crystal was mounted on a glass fiber with epoxy for structure determination. The intensity data sets were corrected with the ω-scan technique. The data were integrated using the CrystalClear program, and the intensities were corrected for Lorentz polarization, air absorption, and absorption attributable to the variation in the path length through the detector faceplate. Absorption corrections based on the Multiscan technique were also applied. All structures were solved by the direct methods and refined by full-matrix least-squares fitting on F^2 using SHELX-97.[44] All non-hydrogen atoms were refined anisotropically except some atoms in $[Pb_4(OH)_4](NO_3)_4$, $Pb_{20}O_6(OH)_{16}(NO_3)_{12}$, $Pb_2O(OH)NO_3$, and $Pb_3O_2(OH)NO_3$, which were refined with "ISOR" constraints. O(49)−O(64) in $[Pb_4(OH)_4](NO_3)_4$, O(1)−O(22), except O(2), O(4), O(5), O(6), O(12), and O(16), in $Pb_{20}O_6(OH)_{16}(NO_3)_{12}$, O(2) in $Pb_2O(OH)NO_3$, and O(3) in $Pb_3O_2(OH)NO_3$ are assigned to be hydroxyl groups on the basis of the requirements of charge balance and bond valence calculations, and their calculated bond valences are in the range 1.29−1.49, 1.22−1.49, 1.19, and 1.13, respectively. The hydrogen atoms in all compounds were not located, and all the largest residual peaks in the final electron density map were close to Pb atoms. All of the structures were verified using the ADDSYM algorithm from the program PLATON,[45] and apart from $Pb_3O_2(OH)NO_3$, no higher symmetries were found in the structures. Relevant crystallographic data and details of the experimental conditions for $Pb_{20}O_6(OH)_{16}(NO_3)_{12}$, $Pb_2O(OH)NO_3$, and $Pb_3O_2(OH)NO_3$ are summarized in Table 1. Atomic coordinates and isotropic displacement coefficients are listed in Tables S1−S4 (Supporting Information) and bond lengths in Tables S5−S8 (Supporting Information).

Table 1. Crystal Data and Structure Refinement for $Pb_{20}O_6(OH)_{16}(NO_3)_{12}$, $Pb_2O(OH)NO_3$, and $Pb_3O_2(OH)NO_3$[a]

formula	$Pb_{20}O_6(OH)_{16}(NO_3)_{12}$	$Pb_2O(OH)NO_3$	$Pb_3O_2(OH)NO_3$
fw	5256.15	509.41	732.61
cryst syst	triclinic	orthorhombic	orthorhombic
space group	$P\bar{1}$	*Pbca*	*Pbcm*
a (Å)	8.594(7)	5.969(8)	8.765(5)
b (Å)	14.601(13)	11.931(17)	14.126(9)
c (Å)	23.91(2)	14.45(2)	5.714(3)
α (deg)	97.277(10)	90	90
β (deg)	98.222(14)	90	90
γ (deg)	91.758(8)	90	90
V (Å^3)	2942(4)	1029(2)	707.5(7)
Z	2	8	4
ρ(calcd) (g/cm ^{3})	5.915	6.563	6.869
T (K)	293(2)	293(2)	293(2)
λ (Å)	0.71073	0.71073	0.71073
F(000)	4376	1688	1203
R/wR ($I > 2\sigma(I)$)	0.0789/0.1932	0.0588/ 0.1808	0.0488/0.1324
R/wR (all data)	0.1044/0.2173	0.0727/0.1875	0.0577/0.1372
GOF on F^2	1.007	1.387	1.128

[a] $R(F) = \Sigma||F_o| - |F_c||/\Sigma|F_o|$. $wR(F_o^2) = [\Sigma w(F_o^2 - F_c^2)^2/\Sigma w(F_o^2)^2]^1$.

Powder X-ray Diffraction. X-ray diffraction patterns of polycrystalline materials were obtained at room temperature on a Rigaku Dmax2500 powder X-ray diffractometer using Cu Kα radiation (λ = 1.540 598 Å) in the angular range 2θ = 5−65° with a scan step width of 0.05° and a fixed time of 0.2 s.

Infrared (IR) Spectroscopy. The FT-IR spectra (KBr pellet) were recorded on an ABB Bomen MB 102 spectrometer in the range 4000−400 cm^{-1}.

dx.doi.org/10.1021/ic5004116 | *Inorg. Chem.* 2014, 53, 5222−5228

UV−Vis Diffuse Reflectance Spectroscopy. UV−vis diffuse reflectance spectra were recorded at room temperature on a powder sample with $BaSO_4$ as a standard (100% reflectance). Data were collected on a PerkinElmer Lamda-900 UV−vis−NIR spectrophotometer scanning in the range 190−2500 nm. Reflectance values were converted to absorbance using the Kubelka−Munk function.[46,47]

Thermal Analysis. Thermogravimetric analysis (TGA) was carried out on a NETZSCH STA 449C unit crystal samples (3−10 mg) that were enclosed in Al_2O_3 crucibles and heated from room temperature to 800 °C at a rate of 10 °C/min under a constant flow of nitrogen gas.

Second-Harmonic Generation. Powder second-harmonic generation (SHG) signals were measured using the method adapted from Kurtz and Perry.[48] Since SHG efficiencies are known to depend strongly on particle size, polycrystalline samples were ground and sieved into the following particle size ranges: 25−45, 45−62, 62−75, 75−109, 109−150, and 150−212 μm. The samples were pressed between glass microscope cover slides and secured with tape in 1-mm thick aluminum holders containing an 8-mm diameter hole. To make relevant comparisons with known SHG materials, crystalline KH_2PO_4 (KDP) samples were also ground and sieved into the same particle size ranges. The samples were then placed in a light-tight box and irradiated with a pulsed laser. The measurements were performed with a Q-switched Nd:YAG laser at the wavelength of 1064 nm. A cutoff filter was used to limit background flash-lamp light on the sample. An interference filter (530 ± 10 nm) was used to select the second harmonic for detection with a photomultiplier tube attached to a RIGOL DS1052E 50-MHz oscilloscope. This procedure was then repeated using the standard nonlinear optical materials KDP, and the ratio of the second-harmonic intensity outputs were calculated. No index-matching fluid was used in any of the experiments.

RESULTS AND DISCUSSION

A simple hydrothermal reaction was employed by using conventional reagent $Pb(NO_3)_2$ as the starting material and NaOH to adjust pH values of the reaction systems. Five different lead hydroxide nitrates, among which $Pb_{20}O_6(OH)_{16}(NO_3)_{12}$ and $Pb_2O(OH)NO_3$ are new, were obtained by this synthetic method. It is worth noting that the pH value in the reaction system has a significant influence on the product crystals. When the pH value of the reaction system is adjusted to about 4−5, colorless rhomboid crystals of $[Pb_4(OH)_4](NO_3)_4$ were obtained in a yield of about 90.0% based on Pb. When the pH value is about 6−7, long striped crystals of $Pb_{20}O_6(OH)_{16}(NO_3)_{12}$ were obtained in a yield of about 95.2%. When the pH value is about 7−8, pale yellow flaky crystals of $Pb_2O(OH)NO_3$ were obtained in a yield of about 96.4%. Experiments of higher pH value for the system have also been carried out. When the pH value of the reaction system is adjusted to about 9−10, transparent polyhedron-shaped crystals of $Pb_{13}O_8(OH)_6(NO_3)_4$ were obtained in a yield of about 82.0%. When the pH value of the reaction system is about 11, colorless thin columnar crystals of $Pb_3O_2(OH)NO_3$, with a small amount of side products, $Pb_{13}O_6(OH)_6(NO_3)_4$ and red powders of PbO, were collected in a yield of about 60.0% based on Pb. When the pH value reached more than 12, only red powders of PbO were obtained. The products obtained with high yield in different final pH values are presented in Chart 1.

Combined with the synthesis conditions of the reaction system for the series of compounds, it is interesting to find the dependence of the ratio of Pb/OH on the pH in the reaction systems (see Chart 2). The deprotonation process of Pb hydroxide groups with the increasing pH value results in the increase of the molar ratio of Pb/OH in molecules of the obtained compounds. The studies of the relationship of pH value and molar ratio of Pb/OH in molecular formula may be

Chart 1. Products Obtained at Different pH Values

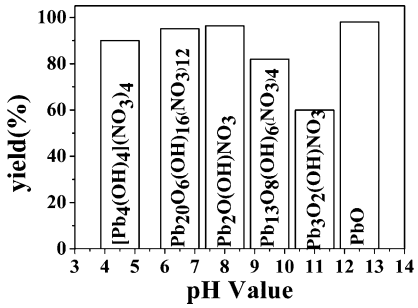

Chart 2. Molar Ratio of Pb/OH under Different pH Values

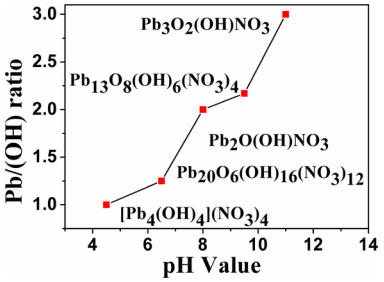

beneficial to the study of detection of lead in drinking water[43] and the transport of Pb from Pb mineral localities to the biosphere.[39] The powder XRD patterns for the pure powder samples showed good agreement with the calculated XRD patterns from the single-crystal models (see Figure S1 in the Supporting Information).

Crystal Structure of $Pb_{20}O_6(OH)_{16}(NO_3)_{12}$. $Pb_{20}O_6(OH)_{16}(NO_3)_{12}$ crystallizes into a monoclinic crystal system with a centrosymmetric space group of $P\bar{1}$. There are 20 unique Pb and 12 N atoms in the structure of $Pb_{20}O_6(OH)_{16}(NO_3)_{12}$. Its unit cell structure is shown in Figure 1a. The structure features infinite cationic chains of $[Pb_{20}O_6(OH)_{16}]_\infty$ (see Figure 1b) running along the c axis, and the nitrate groups as the counterions reside between adjacent chains, which are believed to be responsible for holding the chain structure together mainly through the Pb−O bonds. The chains of $[Pb_{20}O_6(OH)_{16}]_\infty$ make up three kinds of subunits (Figure 1c), namely, distorted cubane cluster $[PbO(OH)_3]$, $[Pb_4O(OH)_2]$ cluster which consist of one (OPb_4) oxocentered tetrahedron and two $[(OH)Pb_2]$ dimers by Pb-O bonds, and slightly distorted trigonal-pyramidal structure of $[PbO(OH)_2]$ in which the lead atom occupies the vertex. In the $[Pb_{20}O_6(OH)_{16}]_\infty$ chain, two inverted trigonal-pyramidal structures of $[PbO(OH)_2]$ connect with the $[Pb_4O(OH)_2]$ cluster in both sides by two Pb−O bonds, respectively, and the cubane cluster $[PbO(OH)_3]$ shares an O atom with one of inverted trigonal-pyramidal structures of $[PbO(OH)_2]$, forming the $[Pb_{10}O_3(OH)_8]$ unit. Two reverse $[Pb_{10}O_3(OH)_8]$ units are linked periodically into the infinite $[Pb_{20}O_6(OH)_{16}]_\infty$ chain. All these polyhedral units are severely distorted owing to the influence of lone pair electrons of the lead(II) cations. The Pb−O bond lengths range from 2.21(2) to 2.76(3) Å, which are close to these reported in the literature.[49,50] The calculated total bond valences for Pb are in the ranges 1.85−2.40 and 4.80−5.43 for the N. Apart from the six O atoms, O(2), O(4), O(5), O(6), O(12), and O(16), which are four coordinated with Pb atoms, O(1)−O(22) are assigned to be hydroxyl groups with the calculated bond valences of 1.22−1.49. In the structure, the

dx.doi.org/10.1021/ic5004116 | Inorg. Chem. 2014, 53, 5222−5228

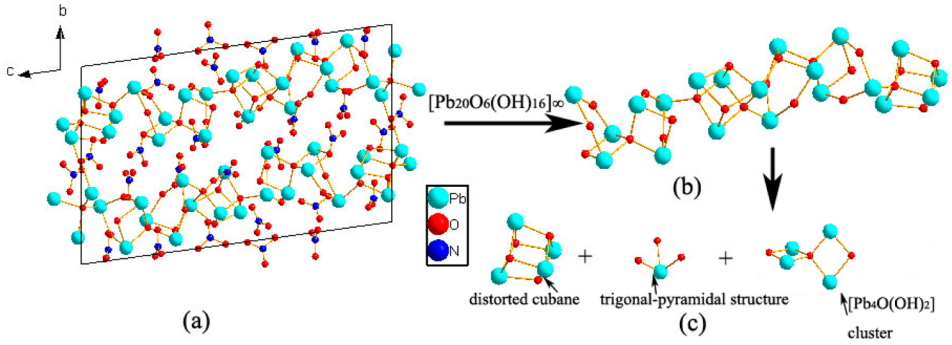

Figure 1. View of the structure of $Pb_{20}O_6(OH)_{16}(NO_3)_{12}$ down the *a* axis (a), 1D chain of $[Pb_{20}O_6(OH)_{16}]_\infty$ (b), and the subunits of distorted cubane, $[Pb_4O(OH)_2]$ cluster, and trigonal-pyramidal structures for composition of 1D chain (c).

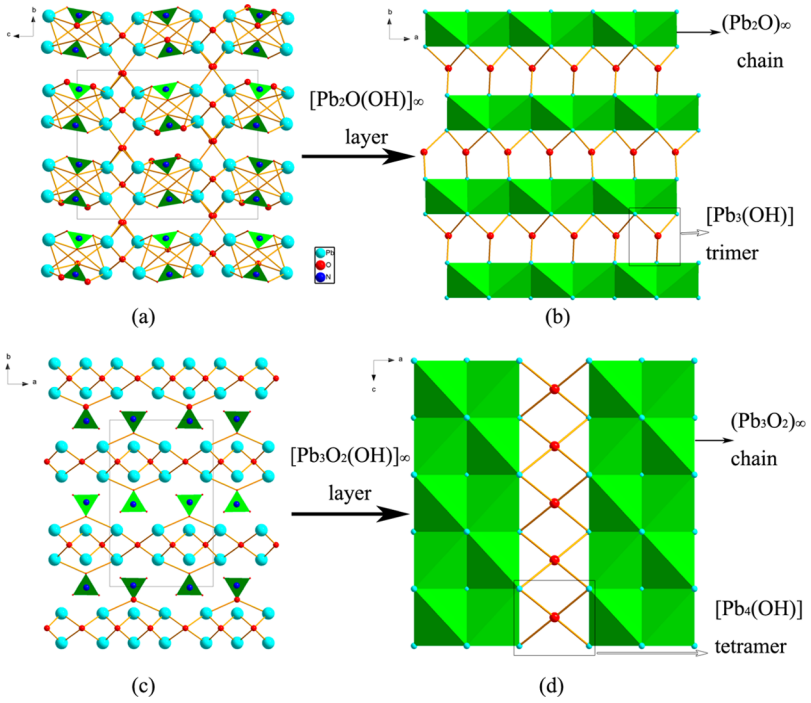

Figure 2. Unit cell structures for $Pb_2O(OH)NO_3$ (a) and $Pb_3O_2(OH)NO_3$ (c), and the layer structures for$[Pb_2O(OH)]_\infty$ (b) and $[Pb_3O_2(OH)]_\infty$ (d).

nitrate anions are disordered, oriented between the $[Pb_{20}O_6(OH)_{16}]_\infty$ chains. Some of these nitrate groups are slightly distorted. The N atoms are coordinated to three O atoms to form planar $[NO_3]$ triangles, and the average N−O bond length is 1.23(4).

Crystal Structure of $Pb_2O(OH)NO_3$ and $Pb_3O_2(OH)NO_3$. $Pb_2O(OH)NO_3$ crystallizes in the centrosymmetric space group *Pbca*. As shown in Figure 2a, the structure can be described as alternate stacking of cationic $[Pb_2O(OH)]_\infty$ layers with layers of NO_3 groups along the *c* axis by the weak Pb−O bonds only, forming a 3D framework with 1D tunnels of 12-member rings (MRs). Seen from the *c* axis (Figure 2b), the $[Pb_2O(OH)]_\infty$ layers can be described as the interconnection of $(Pb_2O)_\infty$ chains of edge-sharing (Pb_4O) tetrahedras by OH^- in the $Pb_3(OH)$ trimer. Each individual OH^- serves as a common vertex for three Pb atoms. In the structure, the N atoms are coordinated to three O atoms to form planar $[NO_3]$ triangles with N−O bond lengths ranging from 1.22(4) to 1.23(4) Å. The $[NO_3]$ triangles have different kinds of orientations which are not in the same plane. The symmetric unit of $Pb_2O(OH)NO_3$ contains two unique lead atoms and one nitrogen atom. Both Pb(1) and Pb(2) are seven coordinated with six O atoms and one $[OH]^-$ group, respectively. The bond lengths for Pb−O are in the range 2.272(18)−3.18(5) Å. These $[Pb(1)O_6(OH)]$ and $[Pb(2)O_6(OH)]$ polyhedra are highly distorted owing to the lone pair electrons of the lead(II) cations. The O(2) atom is assigned to be that of the hydroxyl group with the calculated bond valence of 1.19. The calculated total bond valences for Pb(1) and Pb(2) are 1.95 and 1.97, respectively, and 5.28 for N(1), which are in good agreement with the expected valence states.

The structure of $Pb_3O_2(OH)NO_3$ was reported with an acentric space group, $Pca2_1$.[40] However, according to the X-ray single crystal structural analyses, the structure of $Pb_3O_2(OH)NO_3$ was confirmed to be with the centrosymmtric space group, *Pbcm*. Besides, it was further proved by the SHG measurement which showed that $Pb_3O_2(OH)NO_3$ is without NLO effect. The unit cell structure for $Pb_3O_2(OH)NO_3$ is showen in Figure 2c. Its $[Pb_3O_2(OH)]_\infty$ layers (Figure 2d) parallel to (010) are separated by layers of NO_3 groups, in

dx.doi.org/10.1021/ic5004116 | *Inorg. Chem.* 2014, 53, 5222−5228

which the planes of the NO_3 triangles are parallel to the (001). There are weak bonds between the Pb atoms and the O atoms of the NO_3 groups. The crystal structure of $Pb_3O_2(OH)NO_3$ contains three unique Pb atoms, one unique N atom, six unique O atoms, and one H atom. All atoms are in special positions, a fact that certainly explains the difficulties encountered during the structure solution. As the calculated bond valence sum for O(3) amounts to 1.13, it is assigned to the OH group. The bond lengths for Pb−O are in the range 2.257(11)−3.090(9) Å, and the distances for Pb−OH vary from 2.573(17) to 2.589(17) Å and from 1.21(3) to 1.30(4) Å for N−O.

It is worth comparing the layerd structure of $Pb_2O(OH)NO_3$ with that of $Pb_3O_2(OH)NO_3$. The apparent difference is the pH value of the synthesis system which results in the differences in the structures. The $(Pb_3O_2)_\infty$ chains of edge-sharing (OPb_4) tetrahedral in the structure of $Pb_3O_2(OH)NO_3$ are interconnected by $[Pb_4(OH)]$ tetramer, forming the $[Pb_3O_2(OH)]_\infty$ layers which extend along the (010) plane, while the $[Pb_2O(OH)]_\infty$ layers for $Pb_2O(OH)NO_3$ are formed by the interconnection of (Pb_2O) chains by OH^- in the $[Pb_3(OH)]$ trimer along (001) (Figure 2b,d). Besides, the orientations of nitrate groups in these two structures are various. The NO_3 triangles are approximately perpendicular to the *c* axis and have two kinds of orientations in the structure of $Pb_3O_2(OH)NO_3$, while the NO_3 triangles for $Pb_2O(OH)NO_3$ are approximate parallel to the (001) plane but also have two opposite orientations. All these differences for these two compounds above have attracted our attention to the relationship between crystal structures and pH value.

On the basis of the above structural description, the structures for these series of basic lead nitrates present each feature, such as $[Pb_4(OH)_4](NO_3)_4$ with discrete $[Pb_4(OH)_4]^{4+}$ clusters, $Pb_{20}O_6(OH)_{16}(NO_3)_{12}$ with infinite $[Pb_{20}O_6(OH)_{16}]_\infty$ chain, $Pb_2O(OH)NO_3$ with $[Pb_2O(OH)]_\infty$ layers, $Pb_3O_2(OH)NO_3$ with $[Pb_3O_2(OH)]_\infty$ layers, and $Pb_{13}O_8(OH)_6(NO_3)_4$ with $[Pb_{13}O_8(OH)_6]^{4+}$ clusters.[39] A characterization can be found that all these clusters consist of some of these groups, (OPb_4) oxocentered tetrahedron, $[(OH)Pb_2]$ dimer, $[(OH)Pb_3]$ trimer, and $[(OH)Pb_4]$ tetramer. Among these groups, anions (O^{2-} and OH^-) play the role of the central atoms or the bridging groups. O^{2-} locates at the center of tetrahedron defined by Pb^{2+} cations, forming (OPb_4) oxocentered tetrahedrons in all the compounds reported, while OH^- acts as bridging groups. Thus, the coordination geometries of the O^{2-} anions are distinctly different from OH^- anions in this series of lead compounds. The molar ratio between O^{2-} and OH^- resulting from deprotonation of lead(II) hydroxide groups under different pH values in the reaction system leads to the diversity of structures. Ultimately, the apparent difference is the pH value of the synthesis system which results in the diversity in the structures. Thus, the type of lead clusters was determined by the pH value of the lead aqueous solution. With the rise of pH value, the ratio of Pb/OH in the molecular formulas of these compounds increases, leading to the formation of larger clusters.

OPTICAL PROPERTIES

UV−vis diffuse reflectance spectra were collected for $Pb_{20}O_6(OH)_{16}(NO_3)_{12}$ and $Pb_2O(OH)NO_3$. Absorption (K/S) data were calculated from the following Kubelka−Munk function: $F(R) = (1 - R)^2/2R = K/S$, where R is the reflectance, K is the absorption, and S is the scattering. In the (K/S)-versus-E plots, extrapolating the linear part of the rising curve to zero provides the onset of absorption. The UV absorption spectra of $Pb_{20}O_6(OH)_{16}(NO_3)_{12}$ and $Pb_2O(OH)NO_3$ reveal that they show little absorption in the range 344−2500 nm (Supporting Information, Figure S2). Optical diffuse reflectance spectrum studies indicate that the optical band gaps for the three compounds are approximately 3.60 and 3.46 eV, respectively, which indicates that the two compounds are wide band gap semiconductors.[50]

Figure S3 (Supporting Information) presents the IR spectra of $Pb_{20}O_6(OH)_{16}(NO_3)_{12}$ and $Pb_2O(OH)NO_3$. The three figures exhibit some similar characteristics. According to the literature,[22,50,51] for $Pb_{20}O_6(OH)_{16}(NO_3)_{12}$, the broad absorption band at 3456 cm^{-1} can be attributed to the presence of OH^- groups, and the peaks of 1389, 1030, 913, 797, and 692 cm^{-1} can be assigned to the characteristic peaks of nitrate (Supporting Information, Figure S3a). As to $Pb_2O(OH)NO_3$, the peak at 3523 cm^{-1} confirms similarly the presence of OH^- groups, and the peaks at 1351 and 825 cm^{-1} are the characteristic peaks of nitrate (Supporting Information, Figure S3b).

THERMAL PROPERTIES

The thermal behaviors for $Pb_{20}O_6(OH)_{16}(NO_3)_{12}$ and $Pb_2O(OH)NO_3$ are shown in Figure S4 (Supporting Information). TGA studies show that $Pb_{20}O_6(OH)_{16}(NO_3)_{12}$ displays weight loss in two large steps in the range 143−585 °C under nitrogen atmosphere, leading to a total weight loss of about 15.52% (calculated value 15.07%). The first weight loss step of $Pb_{20}O_6(OH)_{16}(NO_3)_{12}$ corresponds to the condensation of 16 hydroxyl groups, showing a weight loss about 2.77% (calculated value 2.74%), and the second step is attributed to the decomposition of 12 nitrate groups, showing a weight loss about 12.75% (calculated value 12.33%) (Supporting Information, Figure S4a). $Pb_2O(OH)NO_3$ undergoes two steps of weight loss in the temperature ranges 134−250 and 250−575 °C due to the condensation of hydroxyl groups and the release of NO_2 and O_2, corresponding to the weight loss of 1.61% (calculated value 1.77%) and 11.03% (calculated value10.60%), respectively (Supporting Information, Figure S4b).

NLO PROPERTIES

The curves of the SHG signal as a function of particle size from the measurements made on ground crystals for $[Pb_4(OH)_4](NO_3)_4$ are shown in Figure 3. The results are consistent with phase-matching behaviors according to the rule proposed by Kurtz and Perry.[52] A KDP sample is selected as a reference. The second-harmonic signal is found to be 0.7 × KDP for $[Pb_4(OH)_4](NO_3)_4$. The value is proportional to the squares of the nonlinear d_{eff} coefficient. Since the reported d_{36} coefficient for KDP is 0.39 pm/V,[53] the derived d_{eff} coefficient for $[Pb_4(OH)_4](NO_3)_4$ is 0.28 pm/ V.

On the basis of the anionic group theory,[54,55] the dipole transition from the cations to the anionic group ($[NO_3]$ in this case) is the off-site transition. Its value is about 1 order smaller than the dipole transition of the intra-atomic transitions within anionic groups. So the contribution to the main SHG coefficients from the anionic group $[NO_3]$ is dominant, which is much larger than that of the charge transfer between the s-states of cations and the p-originated states of anions. Therefore the macroscopic second-order susceptibility $\chi^{(2)}$ may be expressed by eq 1

dx.doi.org/10.1021/ic5004116 | Inorg. Chem. 2014, 53, 5222−5228

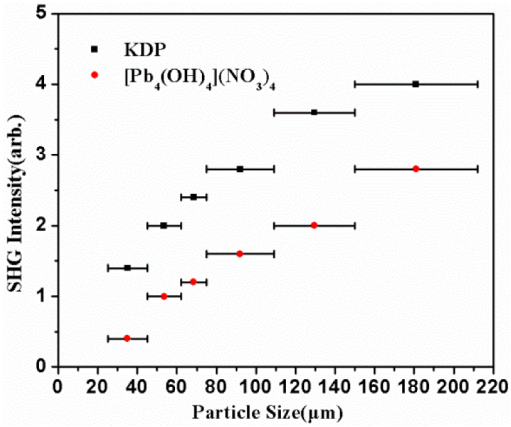

Figure 3. SHG measurements of $[Pb_4(OH)_4](NO_3)_4$ ground crystals (●) with KDP (○) as reference.

$$x_{ijk}^{(2)} = \frac{F}{V}\sum_{p}\sum_{i'j'k'}\alpha_{ii'}\alpha_{jj'}\alpha_{kk'}\beta_{i'j'k'}^{(2)}(\mathrm{P}) \quad \mathrm{P} = [NO_3] \tag{1}$$

where F is the correction factor of the localized field; V is the volume of the unit cell; $\alpha_{ii'}$, $\alpha_{jj'}$, and $\alpha_{kk'}$ are the direction cosines between the macroscopic coordinate axes of the crystal and the microscopic coordinate axes of $[NO_3]^-$ groups; and $\beta_{i'j'k'}$ is the microscopic second-order susceptibility tensors of an individual group. Owing to the fact that $[NO_3]^-$ is a planar group in point group D_{3h}, there are only two nonvanishing second-order susceptibility $\beta_{111}^{(2)} = \beta_{222}^{(2)}$, under the Kleinman approximation. Because the geometrical factor, g, can be derived from eq 2, eq 3 may be simplified according to the deduction process shown in the reference:[56]

$$x_{ijk}^{(2)} = \frac{F}{V}\cdot g_{ijk}\cdot\beta_{111}^{(2)}([NO_3]) \tag{2}$$

In the case of unspontaneous polarization, the structural criterion C is defined as

$$C = \frac{g}{n} \tag{3}$$

where n is the number of anionic groups in a unit cell. The calculated C value was presented in Table 2.

Table 2. Contribution of Different Geometrical Factors (g) for Structure Factors (C)

crystal (n)	$g_{311/n}$	$g_{322/n}$	$g_{333/n}$	$g_{111/n}$	$g_{122/n}$	$g_{133/n}$
$[Pb_4(OH)_4](NO_3)_4$ (n = 64)	0.12	0.04	0.17	0.06	0.07	0.03

Assuming equal localized field (F) on the basis of their similar refractive indices, we know from eqs 2 and 3 that the NLO coefficient $\chi^{(2)}_{ijk}$ is proportional to density of the $[NO_3]^-$ group (n/V) and the structural criterion (C). The $[NO_3]^-$ groups in $[Pb_4(OH)_4](NO_3)_4$ are scattered disorderly, resulting in a small calculated value of the C factor, about 17%, which comes from the contribution of g_{333}. In order to further illustrate the SHG effects as determined by the arrangement of the NLO-active groups and the density of NLO-active groups, the NLO effect of $[Pb_4(OH)_4](NO_3)_4$ was calculated. The small structural criterion value of C factor leads to the small NLO effect, though $[Pb_4(OH)_4](NO_3)_4$ has the moderate density (n/V = 0.0109 Å^{-3}) of the $[NO_3]^-$.

Besides, owing to the Pb^{2+} cation being introduced in the structure, the contribution for the SHG effect of the lone pair electrons of the Pb^{2+} cation was also analyzed by computing the local dipole moments[53,57−59] of PbO_3 polyhedra in the $[Pb_4(OH)_4]^{4+}$ clusters. The direction and magnitude of the 16 kinds of PbO_3 polyhedras in $[Pb_4(OH)_4](NO_3)_4$ are shown in Table S9 (Supporting Information). This shows that the dipole moments along the y axis are cancelled and the values of dipole moments along x and z axis are similar. In order to analyze the contribution of PbO_3 polyhedras in $[Pb_4(OH)_4](NO_3)_4$ for the SHG effect, the $Pb(13)O_3$ with the largest polarization (36.271 D) in the unit cell was chosen as the reference, and then the mean polarizations of PbO_3 polyhedras in the unit cell were used to compare with the largest polarization of $Pb(13)O_3$.The mean polarizations in a unit cell were calculated to be 1.245 D. Compared with the reference, polarization of $Pb(13)O_3$, the mean polarizations are much smaller, 3.432% (the percentage ratio of mean polarizations/largest polarization, 1.247 D/36.271 D). Namely, most of the polarizations of PbO_3 polyhedra in a unit cell were cancelled, which leads to a very small contribution of PbO_3 polyhedras for the SHG effect in $[Pb_4(OH)_4](NO_3)_4$.

Therefore, in light of above two analytical methods, some information can be obtained. Though the NLO effect of $[Pb_4(OH)_4](NO_3)_4$ stems from two kinds of NLO-active groups in the structure, NO_3^- groups and lead oxygen polyhedras, the NLO effect of $[Pb_4(OH)_4](NO_3)_4$ is still relatively small due to the fact that most of the contributions of NLO-active groups are cancelled due to their unfavorable spacial alignment.

CONCLUSION

In summary, a series of lead nitrate specides, among which $Pb_{20}O_6(OH)_{16}(NO_3)_{12}$ and $Pb_2O(OH)NO_3$ are new, have been obtained just by adjusting the pH value of the same reaction system under hydrothermal reaction. Interestingly, with the rise of the pH value, the ratio of Pb/OH in the molecular formula of these compounds increases, which results in the diversity of structures, such as $[Pb_4(OH)_4](NO_3)_4$ with clusters, $Pb_{20}O_6(OH)_{16}(NO_3)_{12}$ with chains, $Pb_2O(OH)NO_3$ and $Pb_3O_2(OH)NO_3$ with layers, and $Pb_{13}O_8(OH)_6(NO_3)_4$ with $[Pb_{13}O_8(OH)_6]^{4+}$ clusters. The acentric crystal $[Pb_4(OH)_4](NO_3)_4$ presents an SHG effect of 0.7 × KDP, which originates from the cooperative effect of NO_3 groups and lead oxygen polyhedras in the structure, and the reasons for the small SHG effect have been presented according to the theoretical analysis. The future research efforts will continue to be focused on the explorations of nitrates, especially those with NLO effects.

ASSOCIATED CONTENT

Supporting Information

Crystal data (CIF), direction and magnitude of PbO_3 polyhedras in $[Pb_4(OH)_4](NO_3)_4$, calculated and experimental XRD patterns, UV absorption spectra and optical diffuse reflectance spectra, IR and TG traces, computational descriptions, theoretical calculations, calculated band structure, and total and partial densities of states for $[Pb_4(OH)_4](NO_3)_4$. This material is available free of charge via the Internet at http://pubs.acs.org.

dx.doi.org/10.1021/ic5004116 | Inorg. Chem. 2014, 53, 5222−5228

AUTHOR INFORMATION

Corresponding Author

*E-mail: nye@fjirsm.ac.cn.

Notes

The authors declare no competing financial interest.

ACKNOWLEDGMENTS

This research was supported by the National Natural Science Foundation of China (Nos. 91222204 and 90922035), Main Direction Program of Knowledge Innovation of Chinese Academy of Sciences (Grant KJCX2-EW-H03-03), and Special Project of National Major Scientific Equipment Development of China (No. 2012YQ120060).

REFERENCES

(1) Chen, C. T; Wang, Y. B.; Wu, B. C.; Wu, K. C.; Zeng, W. L.; Yu, L. H. *Nature* **1995**, *373*, 322−324.
(2) Chen, C. T.; Wu, B. C.; Jiang, A. D.; You, G. M. *Sci. Sin., Ser. B.* **1985**, *28*, 235−243.
(3) Becker, P. *Adv. Mater.* **1998**, *10*, 979−992.
(4) Hagerman, M. E.; Poeppelmeier, K. R. *Chem. Mater.* **1995**, *7*, 602−621.
(5) Wu, H. P.; Pan, S. L.; Poeppelmeier, K. R.; Li, H. Y.; Jia, D. Z.; Chen, Z. H.; Fan, X. Y.; Yang, Y.; Rondinelli, J. M.; Luo, H. S. *J. Am. Chem. Soc.* **2011**, *133*, 7786−7790.
(6) Dmitriev, V. G.; Gurzadyan, G. G.; Nikogosyan, D. N. *Handbook of Nonlinear Optical Crystals*; Springer: Berlin,1991.
(7) Boyd, G. D.; Buehler, E.; Storz, F. G. *Appl. Phys. Lett.* **1971**, *18*, 301−304.
(8) Liao, J. H.; Marking, G. M.; Hsu, K. F.; Matsushita, Y.; Ewbank, M. D.; Borwick, R.; Cunningham, P.; Rosker, M. J.; Kanatzidis, M. G. *J. Am. Chem. Soc.* **2003**, *125*, 9484−9493.
(9) Zhang, Q.; Chung, I.; Jang, J. I.; Ketterson, J. B.; Kanatzidis, M. G. *J. Am. Chem. Soc.* **2009**, *131*, 9896−9897.
(10) Wang, S. C.; Ye, N.; Li, W.; Zhao, D. *J. Am. Chem. Soc.* **2010**, *132*, 8779−8786.
(11) Yu, H. W.; Wu, H. P.; Pan, S. L.; Yang, Z. H.; Su, X.; Zhang, F. F. *J. Mater. Chem.* **2012**, *22*, 9665−9670.
(12) Huang, H. W.; Liu, L. J.; Jin, S. F.; Yao, W. J; Zhang, Y. H.; Chen, C. T. *J. Am. Chem. Soc.* **2013**, *135*, 18319−18322.
(13) Wang, S. C.; Ye, N. *J. Am. Chem. Soc.* **2011**, *133*, 11458−11461.
(14) Xu, X.; Hu, C. L.; Kong, F.; Zhang, J. H.; Mao, J. G.; Sun, J. L. *Inorg. Chem.* **2013**, *52*, 5831−5837.
(15) Huang, H. W.; Yao, J. Y.; Lin, Z. S.; Wang, X. Y.; He, R.; Yao, W. J.; Zhai, N. X; Chen, C. T. *Angew. Chem., Int. Ed.* **2011**, *123*, 10456−10456.
(16) Chen, C. T.; Wu, Y. C.; Jiang, A. D.; Wu, B. C.; You, G. M.; Li, R. K.; Lin, S. J. *J. Opt. Soc. Am. B* **1989**, *6*, 616−621.
(17) Mei, L. F.; Wang, Y. B.; Chen, C. T.; Wu, B. C. *J. Appl. Phys.* **1993**, *74*, 7014−7015.
(18) Zou, G. H.; Huang, L.; Ye, N.; Lin, C. S.; Cheng, W. D.; Huang, H. *J. Am. Chem. Soc.* **2013**, *135*, 18560−18566.
(19) Zou, G. H.; Ye, N.; Huang, L.; Lin, X. S. *J. Am. Chem. Soc.* **2011**, *133*, 20001−20007.
(20) Luo, M.; Ye, N.; Zou, G. H.; Lin, C. S.; Cheng, W. D. *Chem. Mater.* **2013**, *25*, 3147−3153.
(21) Tran, T. T.; Halasyamani, P. S. *Inorg. Chem.* **2013**, *52*, 2466−2473.
(22) Wang, C. P.; Liu, Q.; Li, Z. H. *Cryst. Res. Technol.* **2011**, *46*, 655−658.
(23) Held, P.; Hellwig, H.; Ruhle, S.; Bohaty, L. *J. Appl. Crystallogr.* **2000**, *33*, 372−379.
(24) Halasyamani, P. S.; Poeppelmeier, K. R. *Chem. Mater.* **1998**, *10*, 2753−2769.
(25) Ye, H. Y.; Fu, D. W.; Zhang, Y.; Zhang, W.; Xiong, R. G.; Huang, S. D. *J. Am. Chem. Soc.* **2008**, *131*, 42−43.
(26) Ra, H. S.; Ok, K. M.; Halasyamani, P. S. *J. Am. Chem. Soc.* **2003**, *125*, 7764−7765.
(27) Sykora, R. E.; Ok, K. M.; Halasyamani, P. S.; Albrecht-Schmitt, T. E. *J. Am. Chem. Soc.* **2002**, *124*, 1951−1957.
(28) Chi, E. O.; Ok, K. M.; Porter, Y.; Halasyamani, P. S. *Chem. Mater.* **2006**, *18*, 2070−2074.
(29) Zhang, W. L.; Cheng, W. D.; Zhang, H.; Geng, L.; Lin, C. S.; He, Z. Z. *J. Am. Chem. Soc.* **2010**, *132*, 1508−1509.
(30) Inaguma, Y.; Yoshida, M.; Katsumata, T. *J. Am. Chem. Soc.* **2008**, *130*, 6704−6705.
(31) Phanon, D.; Gautier-Luneau, I. *Angew. Chem., Int. Ed.* **2007**, *46*, 8488−8491.
(32) Huang, Y. Z.; Wu, L. M.; Wu, X. T.; Li, L. H.; Chen, L.; Zhang, Y. F. *J. Am. Chem. Soc.* **2010**, *132*, 12788−12789.
(33) Sun, C. F.; Hu, C. L.; Xu, X.; Ling, J. B.; Hu, T.; Kong, F.; Long, X. F.; Mao, J. G. *J. Am. Chem. Soc.* **2009**, *131*, 9486−9487.
(34) Britton, H. T. S.; Meek, F. H. *J. Chem. Soc.* **1932**, 183−196.
(35) Pauley, J. L.; Testerman, M. K. *J. Am. Chem. Soc.* **1954**, *76*, 4220−4222.
(36) Kwestroo, W.; Langereis, C.; van Hal, H. A. M. *J. Inorg. Nucl. Chem.* **1967**, *29*, 33−38.
(37) Grimes, S. M.; Johnston, S. R.; Abrahams, I. *J. Chem. Soc., Dalton Trans.* **1995**, *12*, 2081−2086.
(38) Li, Y. P.; Krivovichev, S. V.; Burns, P. C. *J. Solid State Chem.* **2000**, *153*, 365−370.
(39) Li, Y. P.; Krivovichev, S. V.; Burns, P. C. *J. Solid State Chem.* **2001**, *158*, 74−77.
(40) Krivovichev, S. V.; Li, Y. P.; Burns, P. C. *J. Solid State Chem.* **2001**, *158*, 78−81.
(41) Kolitsch, U.; Tillmanns, E. *Mineral. Mag.* **2003**, *67*, 79−93.
(42) Berdonosov, P. S.; Dolgikh, V. A.; Popovkin, B. A. *Mater. Res. Bull.* **1996**, *31*, 717−722.
(43) Jensen, J. O. *THEOCHEM* **2002**, *587*, 111−121.
(44) Sheldrick, G. M. *Acta Crystallogr., Sect. A* **2008**, *64*, 112−122.
(45) Spek, A. *J. Appl. Crystallogr.* **2003**, *36*, 7−13.
(46) Wendlandt, W. M.; Hecht, H. G. *Reflectance Spectroscopy*; Interscience: New York, 1966.
(47) Tauc, J. *Mater. Res. Bull.* **1970**, *5*, 721−729.
(48) Kurtz, S. K.; Perry, T. T. *J. Appl. Phys.* **1968**, *39*, 3798−3813.
(49) Tran, D. T.; Zavalij, P. Y.; Oliver, S. R. J. *J. Am. Chem. Soc.* **2002**, *124*, 3966−3969.
(50) Song, J. L.; Hu, C. L.; Xu, X.; Kong, F.; Mao, J. G. *Inorg. Chem.* **2013**, *52*, 8979−8986.
(51) Li, Y.; Krivovichev, S. V.; Burns, P. C. *J. Solid State Chem.* **2000**, *153*, 365−370.
(52) Kurtz, S. K. P.; T., T *J. Appl. Phys.* **1968**, *39*, 3798−3813.
(53) Eckardt, R. C.; Masuda, H.; Fan, Y. X.; Byer, R. L. *IEEE J. Quantum Electron.* **1990**, *26*, 922−933.
(54) Chen, C. T. *Sci. Sin. (Engl. Ed.)* **1979**, *22*, 756−776.
(55) Chen, C. T.; Liu, G. Z. *Annu. Rev. Mater. Res.* **1986**, *16*, 203−243.
(56) Ye, N.; Chen, Q. X.; Wu, B. C.; Chen, C. T. *J. Appl. Phys.* **1998**, *84*, 555−558.
(57) Godby, R. W.; Schluter, M.; Sham, L. J. *Phys. Rev. B: Condens. Matter Mater. Phys.* **1987**, *36*, 6497−6500.
(58) Terki, R.; Bertrand, G.; Aourag, H. *Microelectron. Eng.* **2005**, *81*, 514−523.
(59) Sun, C. F.; Hu, C. L.; Mao, J. G. *Chem. Commun* **2012**, *48*, 4220−4222.